Volume 11 | Number 10 | 21 May 2024

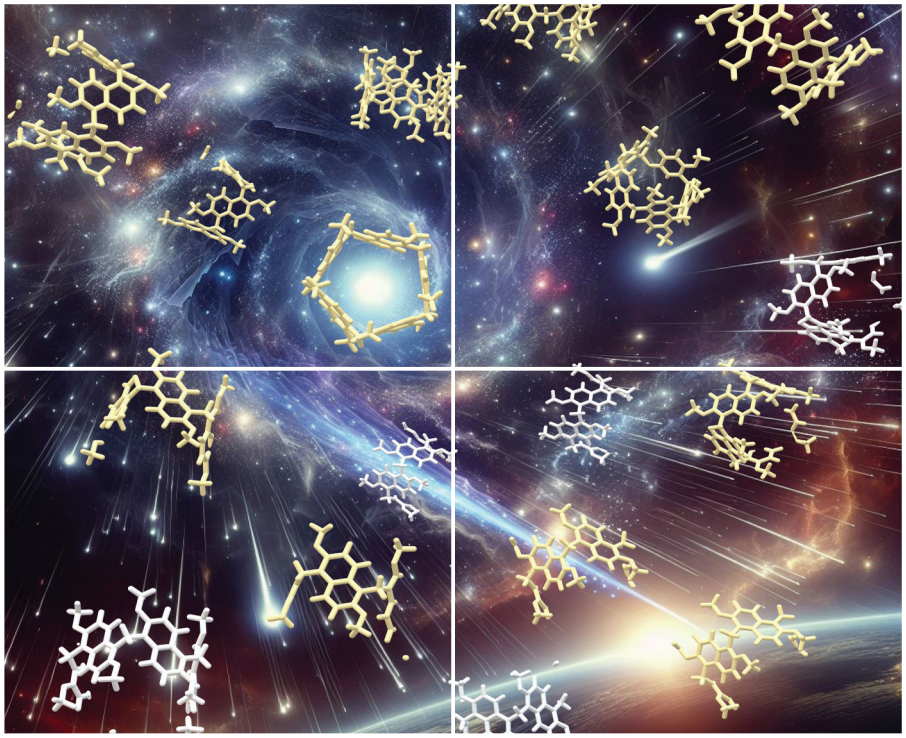

ORGANIC CHEMISTRY

FRONTIERS

CCS 中国化学会 CHINESE CHEMICAL SOCIETY

SIOC 1950

ROYAL SOCIETY OF CHEMISTRY

rsc.li/frontiers-organic

ORGANIC CHEMISTRY FRONTIERS

RESEARCH ARTICLE

View Article Online
View Journal | View Issue

Cite this: *Org. Chem. Front.*, 2024, **11**, 2710

Synthesis, conformational properties, and molecular recognition abilities of novel prism[5]arenes with branched and bulky alkyl groups†

Rocco Del Regno, [a] Paolo Della Sala, [a] Ivan Vollono, [a] Carmen Talotta, [a] Placido Neri, [a] Neal Hickey, [b] Siddharth Joshi, [b] Silvano Geremia *[b] and Carmine Gaeta *[a]

Received 29th December 2023,
Accepted 20th February 2024

DOI: 10.1039/d3qo02139d

rsc.li/frontiers-organic

The direct macrocyclization to prism[5]arenes of 2,6-dialkoxynaphthalenes with branched and bulky alkyl groups has been obtained in good yields in the presence of 1,4-dihexyl-DABCO template. These novel prism[5]arenes exhibit typical D_5-symmetry and DFT calculations indicate that the homochiral all-p*S* (all-p*R*) conformation is the most stable of all the possible conformations. Prism[5]arenes crystallize as racemic mixtures (all-p*S*/all-p*R*) in centrosymmetric space groups. The eight crystal structures show C_2 point symmetry of the macrorings, with a larger opening of the cavity observed for **PrS[5]^{iBu}**, **PrS[5]^{MeCy}** and the β-form of **PrS[5]^{PrCy}**. The dynamic stereochemical inversion (from p*R* to p*S* and *vice versa*) of prism[5]arenes was examined by ^{1}H VT NMR experiments. The racemization of prism[5]arene derivatives occurs by through the-annulus-rotation of the naphthalene units. With increasing length of linear alkyl substituents from C2 to C9, the chains tend to pack at both rims, thereby diminishing the conformational freedom of the naphthalene units. The presence of branched alkyl groups at both rims of the prism[5]arenes increases the energy barrier to racemization and consequently lowers the rate of the racemization process. Prism[5]arenes bearing branched or bulky alkyl groups at both rims can form *endo*-cavity complexes with 1,4-dihexyl-DABCO $\mathbf{2}^{2+}$ and piperazonium $\mathbf{3}^{2+}$ guests. Two hosts with branched alkyl groups, **PrS[5]^{iPr}** and **PrS[5]^{iBu}**, show guest binding affinities higher than those calculated for the analogous linear **PrS[5]^{nPr}** and **PrS[5]^{nBu}** prism[5]arenes. This result can be justified on the basis of the greater conformational rigidity and preorganization of prism[5]arenes bearing branched groups.

Introduction

The first generation of macrocyclic hosts, such as cryptands,[1] crown ethers,[2] and spherands,[3] were introduced in the 1960s and 1970s by Lehn, Pedersen and Cram. These hosts featured cavities decorated with oxygen atoms and were specifically designed to host spherical alkali-cations. Subsequently, between the 1980s and 1990s, calixarenes,[4] resorcinarenes,[5] and cucurbiturils[6] gained significant popularity due to their facile chemical functionalisation and conformational versatility. In contrast to the first generation of hosts, calixarenes and resorcinarenes exhibit large aromatic cavities capable of hosting small organic molecules.[4,5]

In 2008, Ogoshi introduced pillararenes,[7] macrocycles formed by 1,4-dialkoxybenzene units bridged by methylene groups, marking the advent of the third generation of macrocyclic hosts. Unlike calix[4]arene, which adopts a cone-shaped structure, pillararenes feature a distinctive pillar-shaped cavity. The rigid structure of pillararenes, along with their unique supramolecular properties, paved the way for the design of a plethora of novel macrocyclic structures, including biphenarenes,[8] oxatubarenes,[9] saucerarenes,[10] pagodarenes,[11] calix[2]naphth[2]arene,[12] and naphthotubes,[13] all characterized by biomimetic deep aromatic cavities.

In this regard, in 2020 we reported a novel class of macrocyclic hosts named prism[*n*]arenes[14] **PrS[*n*]^{R}** (*n* = 5 and 6, in Fig. 1). These prismarenes are constituted by 1,5-methylene bridged 2,6-dialkoxynaphthalene units (Fig. 1). Prismarenes exhibit a deep π-electron rich aromatic cavity[14–19] and can form *endo*-cavity complexes with ammonium guests, both in organic[14–17] and aqueous media. These complexes are stabilized by cation···π and C–H···π interactions.[18]

As a result of these appealing properties, prismarenes have attracted significant interest in the scientific community over the last three years.[20–26] An intriguing aspect of prismarenes

[a]*Dipartimento di Chimica e Biologia "A. Zambelli". Università di Salerno, Via Giovanni Paolo II, I-84084 Fisciano, Salerno, Italy. E-mail: cgaeta@unisa.it*
[b]*Centro di Eccellenza in Biocristallografia, Dipartimento di Scienze Chimiche e Farmaceutiche, Università di Trieste, Via L. Giorgieri 1, I-34127 Trieste, Italy. E-mail: sgeremia@units.it*

†Electronic supplementary information (ESI) available. CCDC 2251128 and 2308578–2308584. For ESI and crystallographic data in CIF or other electronic format see DOI: https://doi.org/10.1039/d3qo02139d

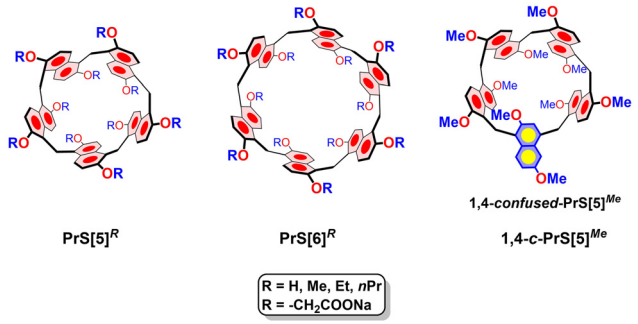

Fig. 1 Chemical drawings of prismarene macrocycles.

pertains to their chirality. Like pillararenes,[27–29] prism[*n*]arenes exhibit planar chirality (Fig. 2). The *pS* and *pR* conformational isomers of the permethylated prismarenes can undergo interconversion *via oxygen-through-the-annulus passage* of the naphthalene units, a process observed to be fast on the NMR time scale (Fig. 2).[24] To isolate *pS*- and *pR*-enantiomeric forms of prism[5]arenes, it becomes necessary to impede the rotational motion of the naphthalene units. Ogoshi and coworkers demonstrated[27,28] that the presence of bulky and branched groups on both rims of pillar[5]arene is essential to prevent racemization.[27] Their findings revealed that the size and structure of alkyl chains on the rims of pillararenes play a crucial role in this regard. More recently, the chiral and conformational features of prism[5]arenes have been exploited for the chiral recognition of aminoacids.[24] The complexation with chiral guests resulted in strong circular dichroism (CD) signals at the absorption band of prism[5]arenes. Notably, the CD signals induced by the chiral complexation varied with the length of the alkyl chains on the prism[5]arene rims.[24]

Regarding the synthesis of prismarenes, we demonstrated that the direct macrocyclization of 2,6-dimethoxynaphthalene in the presence of 1,4-dihexyl-DABCO as a template yielded **PrS[5]^{Me}** (Fig. 1) as the major product (47%).[14] In contrast, when attempting direct macrocyclization starting from 2,6-diethoxynaphthalene or 2,6-dipropoxynaphthalene in the presence of 1,4-dihexyl-DABCO 2^{2+}, a mixture of **PrS[6]^{R}/PrS[5]^{R}** (R = Et or *n*Pr) was formed.[15] Differently, in the absence of 1,4-dihexyl-DABCO 2^{2+}, the direct macrocyclization delivered the hexamer in very high yields (60–80%) and in short reaction times (30–40 min) in various solvents (cyclohexane, toluene, decaline, chlorocyclohexane).[15] Thus, we concluded that the direct macrocyclization of 2,6-diethoxy or 2,6-dipropoxynaphthalene was driven by an intramolecular thermodynamic self-templating effect,[15] resulting from the self-filling of the internal cavity of the hexamer with ethyl or propyl chains. Both **PrS[6]^{Et}** and **PrS[6]^{nPr}** assumed, in solution and in the solid state, a conformation in which four alkyl chains occupied the cavity of the macrocycle.[15] This self-templating effect drives the direct macrocyclization toward the hexamer, even in the presence of 2^{2+}. These considerations clearly demonstrate that the length of the alkyl chain plays a pivotal role in prismarene synthesis. Consequently, the question arises as to whether direct macrocyclization to prism[5]arene is again favoured in the presence of 1,4-dihexyl-DABCO 2^{2+} when starting from monomers bearing linear C4–C9 alkyl chains (**1a–e** in Scheme 1) or α–δ branched (**1f–h**) groups or even more bulky cyclic substituents (**1j–q**).

In the present study, we report on the direct macrocyclization of 2,6-dialkoxynaphthalenes with alkyl groups of different lengths and structures, resulting in novel prism[5]arene derivatives. Additionally, their conformational properties and molecular recognition abilities have been investigated through NMR studies and X-ray crystallography.

Results and discussion

Synthesis of prism[5]arenes

Initially, we investigated the direct macrocyclization of 2,6-dipentoxynaphthalenes, **1b**, to prism[5]arene (Scheme 1). The reaction utilized 1,4-dihexyl-DABCO 2^{2+} as a template and 1,2-dichloroethane as the solvent. Under the conditions previously

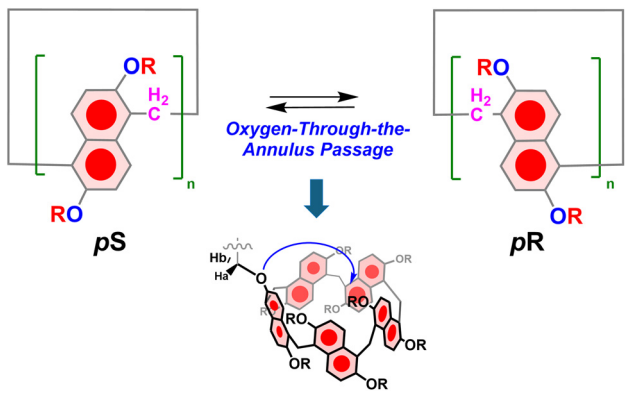

Fig. 2 Planar chirality of prismarenes and racemization process by oxygen-through-the-annulus passage of naphthalene units.

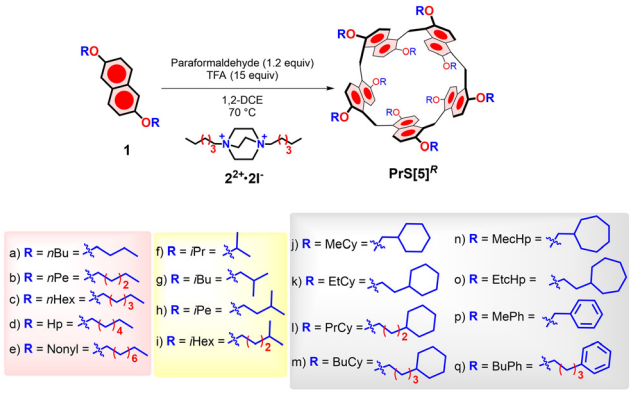

Scheme 1 Direct macrocyclization of 2,6-dialkoxynaphthalene monomers to give prism[5]arene derivatives: 1,2-DCE (5 mM), TFA (15 equiv.), paraformaldehyde (1.2 equiv.), 70 °C, $2^{2+}\cdot 2I^{-}$ (1.0 equiv.).

reported by us,[14,15] a mixture of 2,6-dipentoxynaphthalene **1b**, 1,4-dihexyl-DABCO $\mathbf{2}^{2+}$ (1.0 equiv.), paraformaldehyde (1.2 equiv.) and trifluoroacetic acid (TFA, 15 equiv.) was stirred in 1,2-dichloroethane (1,2-DCE) at 70 °C for 22 h. After purification by column chromatography, the isolated product was identified as 2,6-bis(pentoxy)prism[5]arene, $\mathbf{PrS[5]}^{n\mathbf{Pe}}$, in a yield of 25%. Notably, extending the reaction time to 72 h at 70 °C increased the yield to 35%, and further optimization resulted in a yield of 45% after 120 hours. The structure of $\mathbf{PrS[5]}^{n\mathbf{Pe}}$ was confirmed through 1D and 2D NMR analysis (ESI†), high-resolution mass spectrometry and single crystal X-ray diffraction (ESI† and *vide infra*). The 1D and 2D NMR spectra (CD_2Cl_2, 298 K, 600 MHz) were consistent with the D_5 symmetry previously observed for $\mathbf{PrS[5]}^{\mathbf{Me}}$. Specifically, the ^{1}H NMR spectrum revealed an AX system at 8.31 and 6.95 ppm, corresponding to the aromatic H-atoms of the macrocycle, with a singlet at 4.68 ppm attributable to the methylene-bridges. Encouraged by these results, we extended our investigations to the systematic study of direct macrocyclization of 2,6-dialkoxynaphthalene monomers as a function of alkyl chain length, adding butyl **1a**, hexyl **1c**, heptyl **1d**, and nonyl **1e**.

As indicated in Table 1 (entries 1–4), the direct macrocyclization of **1a**, **1c**, **1d** and **1e** to prism[5]arenes occurred in good yields in the presence of the template 1,4-dihexyl-DABCO $\mathbf{2}^{2+}$ cation. The NMR spectral features of all these prism[5]arenes are consistent with the D_5 symmetry previously observed for other peralkylated prism[5]arene derivatives. Subsequently, a series of experiments were conducted to investigate the effects of branched alkyl groups on the efficiency of the macrocyclization outlined in Scheme 1 (Table 1, entries 6–15). Starting with 2,6-diisopropoxynaphthalene **1f**, the 2,6-bis(isopropoxy)prism[5]arene, $\mathbf{PrS[5]}^{i\mathbf{Pr}}$, was obtained in 48% yield after 24 h. In this case, the formation of the hexamer 2,6-bis(isopropoxy)prism[6]arene, $\mathbf{PrS[6]}^{i\mathbf{Pr}}$,[17] was significant, at a 36% yield even in presence of the template 1,4-dihexyl-DABCO $\mathbf{2}^{2+}$ cation. In fact, the $\mathbf{PrS[6]}^{i\mathbf{Pr}}$ was formed as major product (60%) after 120 h.[17] As recently reported by us,[17] the isopropyl groups can stabilize the cuboid D_2-conformation of the 2,6-bis(isopropoxy)prism[6]arene, $\mathbf{PrS[6]}^{i\mathbf{Pr}}$, through a self-filling effect.[17] Starting with 2,6-diisobutoxynaphthalene **1g**, a $\mathbf{PrS[5]}^{i\mathbf{Bu}}/\mathbf{PrS[6]}^{i\mathbf{Bu}}$ ratio of 3/1 was observed with an overall lower yield. The formation of hexameric prismarene may be attributed to a competitive self-templated effect of the isobutyl chains. However, the situation becomes more complex in this case, as indicated by the crystallographic analysis, revealing that two methyl groups of the isobutyl chains are deeply inserted into the cavity of the pentameric prismarene (see below). The macrocyclization to prism[5]arene was selective with 2,6-diisopentoxynaphthalene **1h** (Table 1, entry 8) and 2,6-diisohexyloxynaphthalene **1i** (Table 1, entry 9), resulting in the formation of the respective prism[5]arene derivatives in 37% and 43% yields, respectively, with no evidence of hexamer in their crude reaction mixtures. Longer isopentyl and isohexyl chains are hypothesized to be less effective in filling the internal cavity of the prism[6]arene, allowing the template effect of $\mathbf{2}^{2+}$ to prevail. Interestingly, the direct macrocyclization of ***1j***, bearing cyclohexylmethyl groups, delivered the prism[5]arene $\mathbf{PrS[5]}^{\mathbf{MeCy}}$ in a 25% yield (Table 1, entry 10), while higher yields were obtained after the direct macrocyclization of **1k** (Table 1, entry 11) and **1l** (Table 1, entry 12) bearing cyclohexylethyl (44%) and cyclohexylpropyl (43%) groups, respectively. These results indicate that, as the cyclohexyl unit gets closer to the rims, the yield of macrocyclization drops significantly (***1k***, 44% → ***1j***, 25%). Analogous results were observed for the direct macrocyclization of **1n** (R = cycloheptylmethyl, Table 1 entry 14) and **1o** (R = cycloheptylethyl, Table 1, entry 15), which gave $\mathbf{PrS[5]}^{\mathbf{MecHp}}$ and $\mathbf{PrS[5]}^{\mathbf{EtcHp}}$ in 30% and 45% yields, respectively. Significantly, the direct macrocyclization of **1p** leads to the formation of 2,6-bis(benzyloxy)prism[5]arene $\mathbf{PrS[5]}^{\mathbf{MePh}}$ in 20% yield (Table 1, entry 16). This prismarene can be considered as a useful precursor of perhydroxylated prism[5]arene.[19] In all the reactions explored in this study (Table 1), the formation of prismarenes with naphthalene units linked at positions 1,4 (confused-prism[5]arenes) was not observed. Typically, the confused-prism[5]arene skeleton adopts a conformation where the 1,4-bridged naphthalene ring is oriented inside the cavity. It is likely that in the presence of long and/or branched alkyl groups, confused-prism[5]arenes cannot be formed, primarily due to the significant steric hindrance caused by these groups within the cavity. Interestingly, the prism[5]arenes bearing long C6–C9 alkyl chains or bulky α–ε branched alkyl groups at both rims, exhibit typical D_5 NMR-patterns. Similar results were observed for prism[5]arene derivatives bearing cyclic units at both rims. Specifically, percyclohexylmethyl-prism[5]arene $\mathbf{PrS[5]}^{\mathbf{MeCy}}$ shows an aromatic AX system at 8.24 and 6.92 ppm with a $\Delta\delta$ value of 1.32 ppm, a value significantly higher than that observed for the 2,6-bis(methoxy)prism[5]arene $\mathbf{PrS[5]}^{\mathbf{Me}}$, which has a $\Delta\delta$ of 1.04 ppm. Similarly, a wide aromatic spacing of 1.44 ppm was observed between the doublets of the 2,6-bis(isobutoxy)prism[5]arene $\mathbf{PrS[5]}^{i\mathbf{Bu}}$. Prism[5]arenes bearing larger cycloheptylmethyl and cycloheptylethyl groups, show aromatic AX systems with a $\Delta\delta$ value of 1.30 and 1.35 ppm, respectively. Also noteworthy is the $\Delta\delta$ value of

Table 1 Synthesis of peralkylated prism[5]arenes $\mathbf{PrS[5]}^{\mathbf{R}}$ (Scheme 1)

Entry	$\mathbf{PrS[5]}^{\mathbf{R}}$	R	Time	Yield (%)
1	$\mathbf{PrS[5]}^{n\mathbf{Bu}}$	*n*-Butyl	120 h	46
2	$\mathbf{PrS[5]}^{n\mathbf{Pe}}$	*n*-Pentyl	120 h	45
3	$\mathbf{PrS[5]}^{n\mathbf{Hex}}$	*n*-Hexyl	120 h	48
4	$\mathbf{PrS[5]}^{\mathbf{Hp}}$	*n*-Heptyl	120 h	35
5	$\mathbf{PrS[5]}^{\mathbf{Nonyl}}$	*n*-Nonyl	120 h	46
6	$\mathbf{PrS[5]}^{\mathbf{iPr}}$	Isopropyl	24 h	48
7	$\mathbf{PrS[5]}^{\mathbf{iBu}}$	Isobutyl	120 h	30
8	$\mathbf{PrS[5]}^{\mathbf{iPe}}$	Isopentyl	120 h	37
9	$\mathbf{PrS[5]}^{\mathbf{iHex}}$	Isohexyl	120 h	43
10	$\mathbf{PrS[5]}^{\mathbf{MeCy}}$	Cyclohexylmethyl	120 h	25
11	$\mathbf{PrS[5]}^{\mathbf{EtCy}}$	Cyclohexylethyl	120 h	44
12	$\mathbf{PrS[5]}^{\mathbf{PrCy}}$	Cyclohexylpropyl	120 h	43
13	$\mathbf{PrS[5]}^{\mathbf{BuCy}}$	Cyclohexylbutyl	120 h	12
14	$\mathbf{PrS[5]}^{\mathbf{MecHp}}$	Cycloheptylmethyl	120 h	30
15	$\mathbf{PrS[5]}^{\mathbf{EtcHp}}$	Cycloheptylethyl	120 h	45
16	$\mathbf{PrS[5]}^{\mathbf{MePh}}$	Benzyl	120 h	20
17	$\mathbf{PrS[5]}^{\mathbf{BuPh}}$	Phenylbutyl	120 h	27

1.41 ppm observed between the aromatic doublets of 2,6-bis (cyclohexylpropyl)prism[5]arene **PrS[5]^{PrCy}**. As previously reported by us,[15] an aromatic $\Delta\delta$ value of 1.30–1.50 ppm suggests that the prism[5]arene skeleton adopts an open conformation[15] in which the aromatic walls exhibit canting angle averaged values close to 90°. Consequently, these results indicate that, in solution, a greater opening of the cavity is observed for **PrS[5]^{iBu}**, **PrS[5]^{MeCy}** and **PrS[5]^{PrCy}**. In this open prismatic conformation, the aromatic H atoms move away from the cavity and experience a down-field shifting with respect to the closed conformation of **PrS[5]^{Me}**, in which a naphthalene ring is folded inside the cavity.

Structural properties of prism[5]arenes in the solid state: the role of the alkyl chains

The crystallographic structures of **PrS[5]^{iPr}**, **PrS[5]^{nBu}**, **PrS[5]^{iBu}**, **PrS[5]^{nPe}**, **PrS[5]^{MeCy}**, **PrS[5]^{EtCy}**, and **PrS[5]^{PrCy}** (α- and β- forms) were determined (Fig. 3a). Details of data collection, structure refinements and geometrical features are reported in the ESI.† All molecules crystallize as racemic mixtures of inherent chiral pairs in centrosymmetric space groups. All prismarene molecules exhibit a similar macrocycle conformation, analogous to the one observed for **PrS[5]^{Me}**, **PrS[5]^{Et}** and **PrS[5]^{nPr}**.[15] The **PrS[5]^{iBu}**, **PrS[5]^{EtCy}** and the α form of **PrS[5]^{PrCy}** show a crystallographic twofold axis passing through the methylene bridge connecting the *C* and *C*′ rings and the middle of the opposite A naphthalene moiety (Fig. S135†). The crystal structures of the other molecules show a pseudo C_2 point symmetry for the **PrS[5]^{R}** scaffold. The canting angles reported in Table S9† illustrate this situation: the dihedral angles of the *B*/*B*′ and *C*/*C*′ couples (see Fig. S135†) are supplementary angles with mean values of 68(2)°/113(2)° for *B*/*B*′ and 136(4)°/44(5)° for *C*/*C*′; while the *A* angle is approximately 90° with a mean value of 89 (1)°. The standard deviations reported in parentheses indicate relatively larger variability in the conformation of the *C*/*C*′ couple with the most fixed position for the A naphthalene. In agreement with NMR studies in solution, a greater opening of the cavity is observed for **PrS[5]^{iBu}**, **PrS[5]^{MeCy}** and the β-form

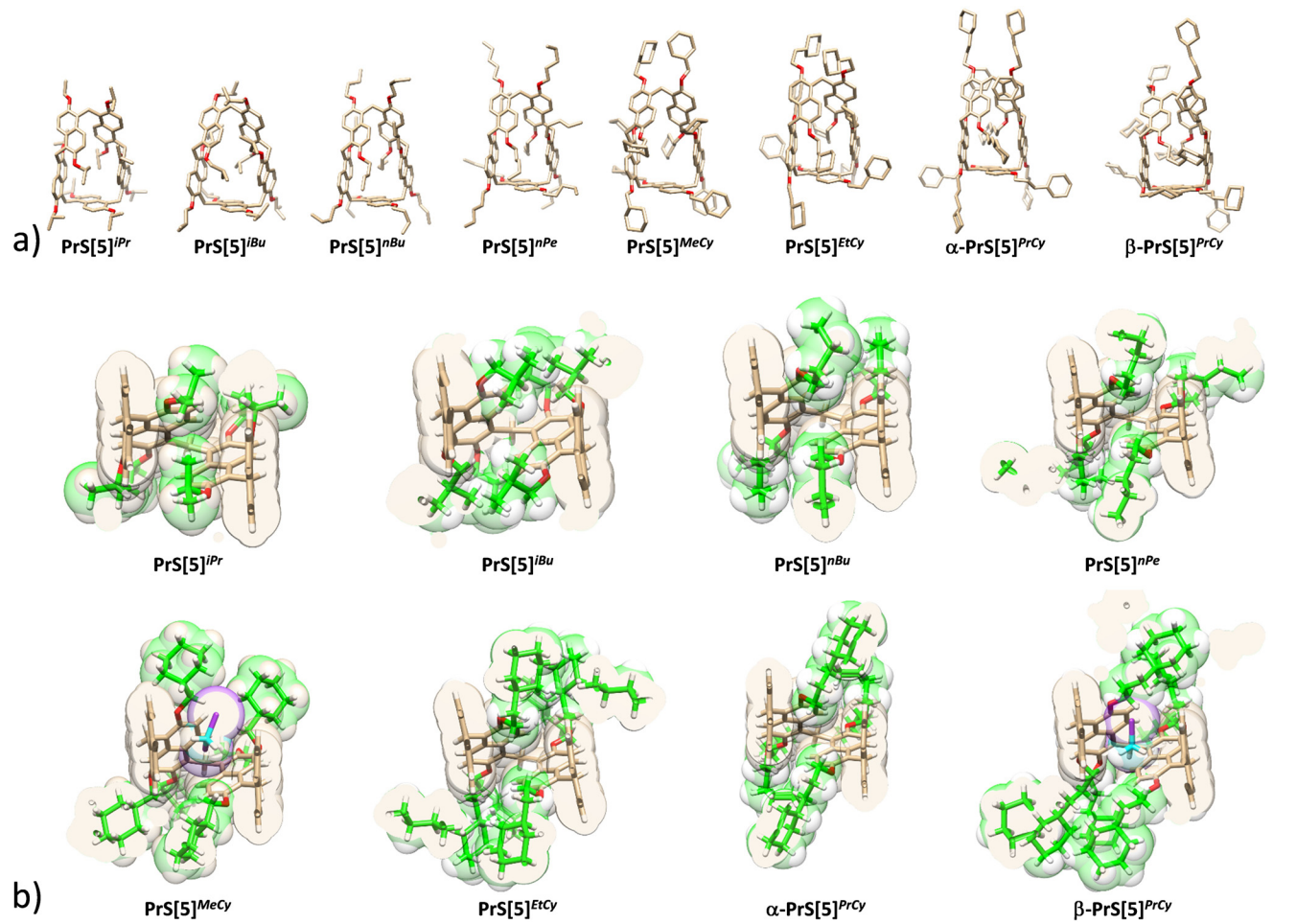

Fig. 3 (a) Stick representation of new **PrS[5]^{R}**. X-ray structures reported in the present work. Hydrogen atoms and solvent molecules are omitted for clarity. For each structure, only one molecule with disordered alkyl groups of highest occupancy is shown. (b) Stick representation with van der Waals surfaces of **PrS[5]^{R}** structures viewed along the C_2 axis. The A naphthalene group in the foreground has been omitted to see the filling of the cavity by alkyl groups (green) or solvent molecules (magenta/cyan).

of **PrS[5]^{PrCy}**, where the *C*/*C*′ angles decrease and increase by about 6°, respectively, in comparison to the other structures (Table S9†). This greater opening is also reflected in the *C*/*C*′ dihedral angles. A mean value of 60(2)° is observed for **PrS[5]^{iBu}**, **PrS[5]^{MeCy}** and β-**PrS[5]^{PrCy}**, while a mean value of 49 (1)° is observed for all the other structures. The opening observed for **PrS[5]^{MeCy}** and β-**PrS[5]^{PrCy}** can be attributed to the presence of a dichloromethane solvent molecule hosted in the prismarene cavity (Fig. 3b). In the case of **PrS[5]^{iBu}**, a self-filling of two symmetry-related methyl groups of the alkoxy chains, one from each C and C′ naphthalene moiety, is observed (Fig. 3b). The analogous **PrS[5]^{iPr}** molecule shows a more closed conformation, with the self-filling of only one methyl group (Fig. 3b). These structural differences in intramolecular interactions could be connected to the differences observed for the product distribution in the synthesis. The other structures all show comparable closed conformations, with the alkoxy chains outside the cavity (Fig. 3b).

Conformational dynamics of prism[5]arenes PrS[5]^{R}

Analogously to pillararene macrocycles, prism[5]arenes exhibit planar chirality (Fig. 2 and 4). The pentamers **PrS[5]^{R}** can adopt 8 conformations of different planar chirality corresponding to 4 enantiomeric pairs (**I–IV** in Fig. 4).

As reported for pillararenes,[27–29] the chirality in these conformational isomers of prism[5]arenes can be described using the p*R* and p*S* nomenclature (Fig. 4).

The stability of the conformational isomers of peralkylated prism[5]arene derivatives was evaluated by DFT calculations at the B97D3/SVP/SVPFIT level of theory (ESI†).[30] The calculations for **PrS[5]^{nPr}**,[15] indicate conformation **I**, all-p*S* (all-p*R*) (Fig. 4), as more stable than all the other possible conformations **II**, **III**, and **IV** by 11.8, 14.7, and 8.1 kcal mol^{-1} (ESI†), respectively.

Analogous results were obtained for the percyclohexylethyl-prism[5]arene **PrS[5]^{EtCy}**: DFT calculations indicate conformation **I** as more stable compared to conformations **II**, **III** and **IV**, by 22.6, 22.9 and 4.4 kcal mol^{-1}, respectively. Similarly, for **PrS[5]^{iPr}**, the all-p*S* (all-p*R*) (Fig. 4), was calculated as more stable than **II**, **III**, and **IV** by 10.0, 11.5, and 6.5 kcal mol^{-1} (ESI†), respectively. The conformational features of the peralkylated prism[5]arene derivatives **PrS[5]^{R}** in Scheme 1 were investigated by variable temperature ^{1}H NMR experiments. The 1D and 2D NMR spectra (25 °C) of the **PrS[5]^{R}** derivatives are in agreement with the D_5 symmetry of their all-p*R* (or all-p*S*) conformation **I**. The presence of diastereotopic resonances attributable to OCH_2 groups in the ^{1}H NMR spectra of 2,6-bis(ethoxy) prism[5]arene (Fig. 5a) and 2,6-bis(propoxy)prism[5]arene at 298 K (300 MHz, Toluene-d_8, ESI†) confirms their planar chirality. As reported in literature for pillar[5]arenes,[27,29,31] the separation of the OCH_2 diastereotopic resonances is a useful probe to study whether racemization of planar chiral macrocycles (Fig. 2 and 5) takes place on the NMR time scale. Racemization processes (Fig. 2) become faster on the NMR time scale as the temperature increases, leading to the coalescence of diastereotopic OCH_2 resonances due to the rapidly averaged chemical environment around OCH_aH_b protons.[27,29,31] Above the coalescence temperature (T_c), the –OCH_2– proton signals generally converge into a sharp singlet (Fig. 5a and b). The presence of diastereotopic resonances attributable to OCH_2 groups of **PrS[5]^{R}** (R = Et, *n*-Pr) indicates that the inversion process between their p*R* and p*S* enantiomeric forms is slow on the NMR time scale, at room temperature. On heating, the diastereotopic OCH_2 signals of **PrS[5]^{Et}** and **PrS[5]^{nPr}** coalesced at 338 K (Fig. 5a) and 348 K (Fig. 5b) (in toluene-d_8), respectively. From these values, energy barriers[32] values of 16.8 and 17.4 kcal mol^{-1} were calculated for the racemization process of **PrS[5]^{Et}** and **PrS[5]^{nPr}**, respectively. Table 2 shows the coalescence temperatures (T_c) and the energy barrier $\Delta G^{\ddagger}$ values for the racemization of prism[5]arene derivatives in Scheme 1. The data in Table 2 clearly indi-

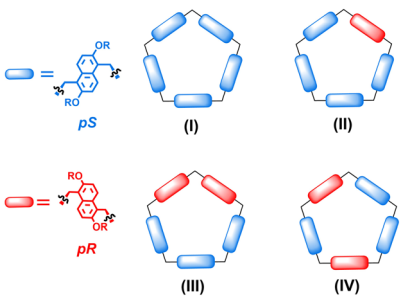

Fig. 4 Schematization of four conformations with different planar chirality **I**–**IV** of a prism[5]arene. (**I**) = p*S*p*S*p*S*p*S*p*S*; (**II**) = p*R*p*S*p*S*p*S*p*S*; (**III**) = p*R*p*R*p*S*p*S*p*S*; (**IV**) = p*R*p*S*p*R*p*S*p*S*. Each conformation has an enantiomer with opposite planar chirality, which results in a total of eight distinct conformations.

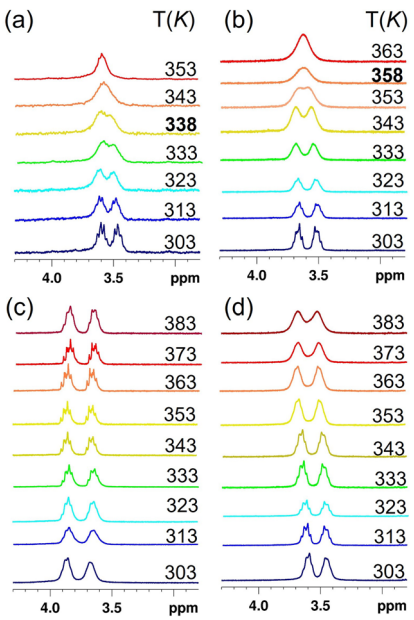

Fig. 5 Partial DNMR spectra of OCH_2 protons: (a) **PrS[5]^{Et}**, (b) **PrS[5]^{nPe}**, (c) **PrS[5]^{EtCy}** and (d) **PrS[5]^{BuPh}** in toluene-d_8.

Table 2 Coalescence temperatures T_C (K) and $\Delta G^{\ddagger}$ (kcal mol^{-1}) values for the oxygen-through-the-annulus rotation of the peralkylated prism[5]arenes **PrS[5]^{R}**

Entry	**PrS[5]^{R}**	R	T_C (K)	$\Delta G^{\ddagger}$ (Kcal mol^{-1})
1	**PrS[5]^{Et}**	Ethyl	338	16.8
2	**PrS[5]^{nPr}**	*n*-Propyl	348	17.4
3	**PrS[5]^{nBu}**	*n*-Butyl	353	17.8
4	**PrS[5]^{nPe}**	*n*-Pentyl	358	18.0
5	**PrS[5]^{nHex}**	*n*-Hexyl	363	18.5
6	**PrS[5]^{Hp}**	*n*-Heptyl	373	18.6
7	**PrS[5]^{Nonyl}**	*n*-Nonyl	[a]	>19.2
8	**PrS[5]^{iPr}**	Isopropyl	[b]	—
9	**PrS[5]^{iBu}**	Isobutyl	373	18.9
10	**PrS[5]^{iPe}**	Isopentyl	373	18.3
11	**PrS[5]^{iHex}**	Isohexyl	383	19.2
12	**PrS[5]^{MeCy}**	Cyclohexylmethyl	[c]	—
13	**PrS[5]^{EtCy}**	Cyclohexylethyl	[b]	—
14	**PrS[5]^{PrCy}**	Cyclohexylpropyl	[b]	—
15	**PrS[5]^{BuCy}**	Cyclohexylbutyl	[b]	—
16	**PrS[5]^{MecHp}**	Cycloheptylmethyl	[b]	—
17	**PrS[5]^{EtcHp}**	Cycloheptylethyl	[b]	—
18	**PrS[5]^{BuPh}**	Phenylbutyl	[b]	—

[a] A broadening of the OCH_2 diastereotopic signals was observed at 383 K. [b] No evidence of coalescence was observed in the temperature range investigated (298–383 K) in toluene-d_8. [c] Deuterated chlorobenzene was used as solvent due to the accidental isochronous appearance of OCH_2 signals in deuterated toluene. In chlorobenzene-d_5 no evidence of coalescence was observed in the temperature range investigated (298–383 K).

cate an increase in the energy barrier $\Delta G^{\ddagger}$ with the increase of the *n*-alkyl chain length from C3 to C9 and thus decreasing the conformational freedom of the macrocycles. Thus, 2,6-bis(nonyloxy)prism[5]arene **PrS[5]^{Nonyl}** showed a broadening of the OCH_2 signals at 383 K, in toluene-d_8 (ESI†) suggesting that rotations of the 2,6-bis(nonyloxy)naphthalene units still occur more slowly than the NMR time scale at this temperature. It seems likely that, with an increase in the length of alkyl substituents, the linear chains pack on both rims, consequently reducing the conformational freedom of the naphthalene units within these prism[5]arenes. The presence of branched alkyl groups at both rims of the prism[5]arenes increases the energy barrier to racemization (Fig. 2) and consequently lowers the rate of the process. In detail, in 2,6-bis(isopropoxy)prism[5]arene **PrS[5]^{iPr}** the diastereotopic $(CH_3)_aCH(CH_3)_b$ signals didn't change their shape even on heating (ESI†). This result clearly indicates that the rotation of the 2,6-bis(isopropoxy)naphthalene units in **PrS[5]^{iPr}** did not take place on the NMR time scale in the temperature range investigated (298–383 K). In contrast, rotation of 2,6-bis(propoxy)naphthalene units in **PrS[5]^{nPr}** is considerably faster. On heating, the diastereotopic OCH_2 signals of **PrS[5]^{nPr}** show a coalescence temperature of 348 K (in toluene-d_8), and an energy barrier of 17.4 kcal mol^{-1} to the racemization process. Similar results were observed for **PrS[5]^{iBu}** and **PrS[5]^{iPe}**, which show coalescence temperatures of 373 K and energy barriers of 18.9 and 18.3 kcal mol^{-1}, respectively, higher than that observed for **PrS[5]^{nBu}** and **PrS[5]^{nPe}**(see Table 2). We have previously shown[17] that 2,6-bis(isopropoxy)prism[6]arene **PrS[6]^{iPr}** exhibits an energy barrier to the racemization process significantly higher than that measured for the isomer 2,6-bis(propoxy)prism[6]arene **PrS[6]^{nPr}**.[15] These results clearly indicate that the presence of branched groups at the rims of prismarene macrocycles increase the energy barrier to the racemization process to a greater extent than the respective isomeric linear groups.

Prompted by these observations, we have investigated the conformational dynamics of prism[5]arenes bearing cyclohexylmethyl (**PrS[5]^{MeCy}**), cyclohexylethyl (**PrS[5]^{EtCy}**), cyclohexylpropyl (**PrS[5]^{PrCy}**), cyclohexylbutyl (**PrS[5]^{BuCy}**), cycloheptylethyl (**PrS[5]^{EtcHp}**), and phenylbutyl groups (**PrS[5]^{BuPh}**) at both rims. In all these cases, the rotation of the respective 2,6-dialkoxynaphthalene units is blocked on the NMR time scale. On heating, the diastereotopic OCH_2 signals of these derivatives didn't show any evidence of broadening in the temperature range investigated (298–383 K, Fig. 5c and d).

To gain insights into the aspect of chiral stability, chiral HPLC studies were carried out for percyclohexylethyl (and percyclohexylpropyl) substituted prism[5]arenes (ESI†). Upon injection of **PrS[5]^{EtCy}** onto a chiral HPLC column, two peaks of equal area were observed in the chromatogram (ESI†). The two enantiomers were collected and reinjected separately. Unfortunately, racemization was again observed after HPLC runs. Analogous results were observed for **PrS[5]^{PrCy}**. Therefore, the chiral prism[5]arene enantiomers are not stable at room temperature, however the chiral separation was observed. This observation is in agreement with the conclusion that the rotation of the 2,6-dicyclohexylethyloxynaphthalene and 2,6-dicyclohexylpropoxynaphthalene units is blocked on the NMR time scale.

Molecular recognition studies

As previously reported by us and others,[11–26] prismarenes form *endo*-cavity supramolecular complexes stabilized by secondary interactions such as cation···π, C–H···π, van der Waals and the hydrophobic effect. Specifically, the **PrS[5]^{R}** (R = Et, *n*Pr)[15] show a high binding affinity toward 1,4-dihexyl-DABCO $\mathbf{2}^{2+}$ and *N*,*N*,*N*′,*N*′-tetramethylpiperazonium $\mathbf{3}^{2+}$ as barfate salts (Table 3 and Fig. 6). Based on these results, we have explored the recognition abilities of some prism[5]arenes obtained in this work. Our aim was to study how the presence of long alkyl chains or branched/bulky groups in **PrS[5]^{R}** can affect the complexation abilities of these new derivatives. When 1,4-dihexyl-DABCO $\mathbf{2}^{2+}$ as barfate salt[33,34] was mixed with 2,6-bis(isopropoxy)prism[5]arene **PrS[5]^{iPr}** in CD_2Cl_2 solution, the ^{1}H NMR spectrum of the host showed significant changes (Fig. 6a–c). The ^{1}H NMR titration experiment in Fig. 6a–c is indicative of an *endo*-cavity complexation process in which chemical exchange between free and complexed species is slow compared to the NMR time scale. In fact, when **PrS[5]^{iPr}** and $\mathbf{2}^{2+}$ were mixed in a 1/0.5 ratio in CD_2Cl_2 solution, the ^{1}H NMR spectrum (Fig. 6b) showed the presence of both, complexed and uncomplexed species. Upon addition of 1 equiv. of $\mathbf{2}^{2+}$ as a barfate salt to a CD_2Cl_2 solution of **PrS[5]^{iPr}** the ^{1}H NMR spectrum (Fig. 6c) showed the presence of the $\mathbf{2}^{2+}$@**PrS[5]^{iPr}** complex alone, while no indication of uncomplexed species

Table 3 Binding constant values for the formation of the complexes between the ammonium 2^{2+} and 3^{2+} cations as barfate salts and **PrS[5]^{Et}**, **PrS[5]^{nPr}**, **PrS[5]^{nBu}**, **PrS[5]^{nPe}**, **PrS[5]^{iPr}**, **PrS[5]^{iBu}**, **PrS[5]^{iPe}**, **PrS[5]^{EtCy}** and **PrS[5]^{EtcHp}**

PrS[5]^{R}	2^{2+} (K_{ass}, M^{-1})	3^{2+} (K_{ass}, M^{-1})
PrS[5]^{Et}	$1.4 \pm 0.2 \times 10^{8}$ M^{-1} [a]	$2.8 \pm 0.4 \times 10^{8}$ M^{-1} [a]
PrS[5]^{nPr}	$1.7 \pm 0.3 \times 10^{8}$ M^{-1} [a]	$1.4 \pm 0.2 \times 10^{9}$ M^{-1} [a]
PrS[5]^{nBu}	$4.6 \pm 0.6 \times 10^{8}$ M^{-1}	$1.1 \pm 0.2 \times 10^{9}$ M^{-1}
PrS[5]^{nPe}	$4.3 \pm 0.6 \times 10^{8}$ M^{-1}	$7.4 \pm 0.9 \times 10^{8}$ M^{-1}
PrS[5]^{iPr}	$3.3 \pm 0.4 \times 10^{9}$ M^{-1} [b]	$1.2 \pm 0.2 \times 10^{10}$ M^{-1} [b]
PrS[5]^{iBu}	$9.6 \pm 0.9 \times 10^{8}$ M^{-1}	$4.3 \pm 0.6 \times 10^{9}$ M^{-1}
PrS[5]^{iPe}	$2.7 \pm 0.4 \times 10^{8}$ M^{-1}	$5.8 \pm 0.8 \times 10^{8}$ M^{-1}
PrS[5]^{EtCy}	$2.1 \pm 0.3 \times 10^{8}$ M^{-1} [b]	$6.8 \pm 0.9 \times 10^{8}$ M^{-1} [b]
PrS[5]^{EtcHp}	$2.1 \pm 0.3 \times 10^{8}$ M^{-1}	$2.8 \pm 0.4 \times 10^{8}$ M^{-1}

[a] See ref. 15. [b] The binding constant obtained by NMR competition experiment is in perfect agreement with the value determined through fluorescence titration experiment. See ESI,† pages S170–173, for further details.

was observed. Thus, the signals at negative values of chemical shifts (−0.64 and −0.97 ppm) in Fig. 6c are attributable to 2^{2+} hosted inside the cavity of **PrS[5]^{iPr}**. In addition, the ^{1}H NMR spectrum of 2^{2+}@**PrS[5]^{iPr}** (Fig. 6c) shows a singlet at 4.79 ppm attributable to $ArCH_2Ar$ groups (4.67 ppm for the free host), a signal at 4.70 ppm for the $OCH(CH_3)_2$ groups and two diastereotopic doublets at 1.59 and 1.30 ppm attributable to methyl groups of $OCH(CH_3)_2$, (1.16 and 0.77 ppm, for the free host). Calculation of the binding constant of the 2^{2+}@**PrS[5]^{iPr}** pseudorotaxane complex, by direct peak integration was not possible as the ^{1}H NMR signals (Fig. 6c) of the host **PrS[5]^{iPr}** and guest 2^{2+} in the unbound forms were undetectable. Following a procedure previously reported by us and other groups, binding constants assessment was carried out by means of a competition experiment in which 1 equiv. of 2^{2+} as a barfate salt was added to a 1 : 1 mixture of 2,6-bis(isopropoxy)prism[5]arene **PrS[5]^{iPr}** and 2,6-bis(propoxy)prism[5]arene **PrS[5]^{nPr}** (in CD_2Cl_2). The 2^{2+}@**PrS[5]^{iPr}** complex was preferentially formed (ESI†), with a percentage of formation of 81% *versus* 19% for 2^{2+}@**PrS[5]^{nPr}**. From these data and knowing the binding constant value of the 2^{2+}@**PrS[5]^{nPr}** complex in CD_2Cl_2, an association constant value of 3.3×10^{9} M^{-1} was calculated (Table 3), significantly higher than that observed for the formation of

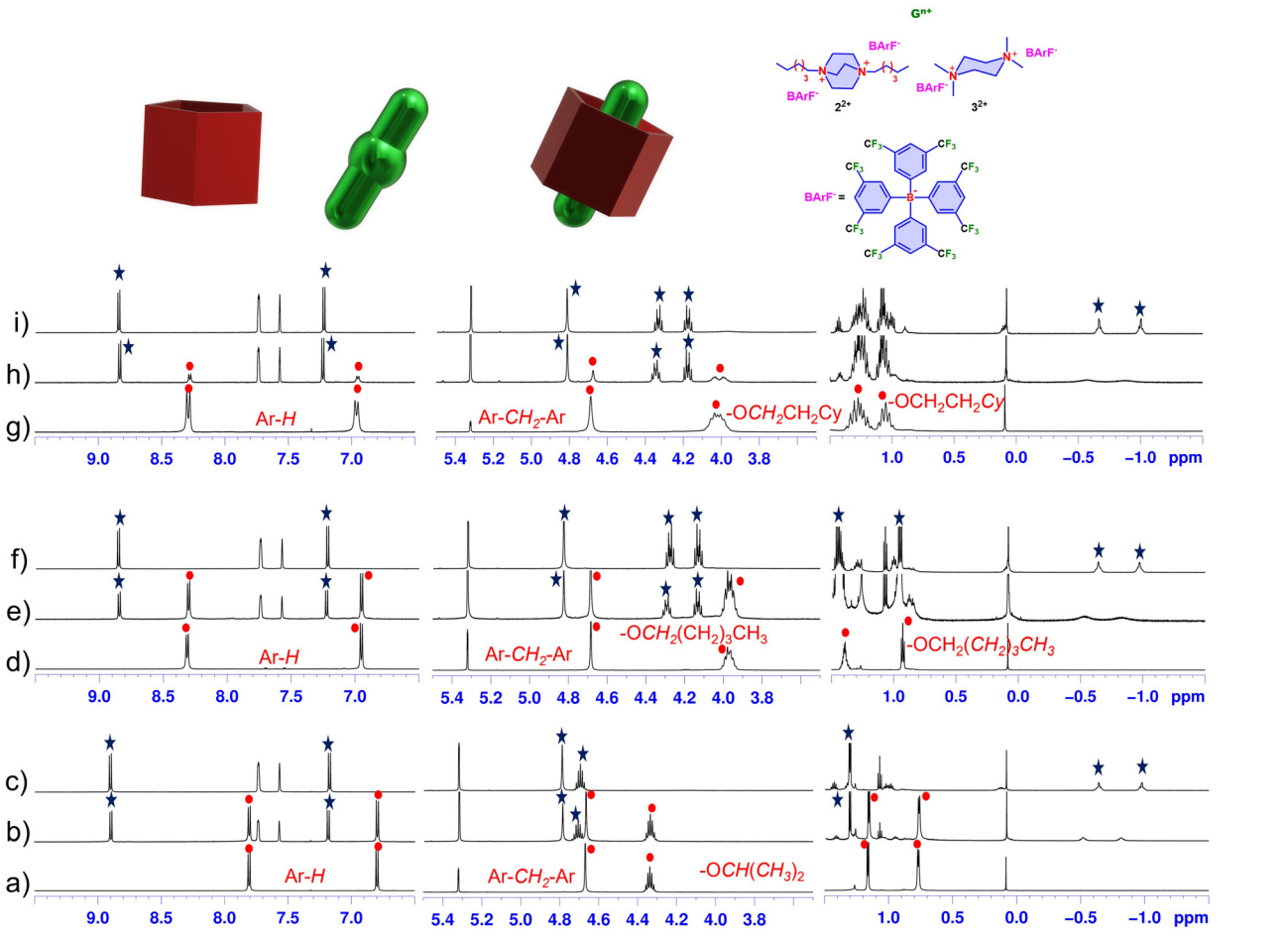

Fig. 6 ^{1}H NMR spectra (CD_2Cl_2, 600 MHz, 298 K) of: (a) **PrS[5]^{iPr}**, (b) a 1 : 0.5 mixture of **PrS[5]^{iPr}** and 2^{2+}·$(BArF)_2$ (2.6 mM), (c) a 1 : 1 mixture of **PrS[5]^{iPr}** and 2^{2+}·$(BArF)_2$ (2.6 mM), (d) **PrS[5]^{nBu}**, (e) a 1 : 0.5 mixture of **PrS[5]^{nBu}** and 2^{2+}·$(BArF)_2$ (2.1 mM), (f) a 1 : 1 mixture of **PrS[5]^{nBu}** and 2^{2+}·$(BArF)_2$ (2.1 mM), (g) **PrS[5]^{EtCy}**, (h) a 1 : 0.5 mixture of **PrS[5]^{EtCy}** and 2^{2+}·$(BArF)_2$ (1.7 mM) and (i) a 1 : 1 mixture of **PrS[5]^{EtCy}** and 2^{2+}·$(BArF)_2$ (1.7 mM). Marked with red circles the signals of free hosts and with blue stars the signals of complexed species.

the $\mathbf{2}^{2+}$@**PrS[5]**^{nPr} complex of 1.7×10^8 M^{-1}. This result can be justified on the basis of the greater conformational rigidity and preorganization of the 2,6-bis(isopropoxy)prism[5]arene **PrS[5]**^{iPr} macrocycle compared to **PrS[5]**^{nPr}. Interestingly, the 2,6-bis(isopropoxy)prism[5]arene **PrS[5]**^{iPr} showed a greater binding affinity toward *N*,*N*,*N*′,*N*′-tetramethylpiperazonium $\mathbf{3}^{2+}$ guest than $\mathbf{2}^{2+}$, with a $\mathbf{3}^{2+}$@**PrS[5]**^{iPr}/$\mathbf{2}^{2+}$@**PrS[5]**^{iPr}selectivity ratio of 3.6 (Table 3).

Analogously, the 2,6-bis(isobutoxy)prism[5]arene **PrS[5]**^{iBu} gives *endo*-cavity complexations in the presence of $\mathbf{2}^{2+}$ and $\mathbf{3}^{2+}$ as barfate salt, with binding affinities higher than those observed for the analogous complexation with 2,6-bis(butoxy) prism[5]arene **PrS[5]**^{nBu} (Table 3). The structure of the *endo*-cavity complex $\mathbf{2}^{2+}$**@PrS[5]**^{iBu}, was investigated by a 2D NOESY experiment (ESI†), revealing diagnostic dipolar couplings between the methylene signals of $\mathbf{2}^{2+}$ shielded inside the cavity of **PrS[5]**^{iBu} at −0.54/−0.85 ppm and the Ar*H* signals of **PrS[5]**^{iBu} at 8.86 and 7.21 ppm (Fig. S105, ESI†), confirming the formation of the *endo*-cavity $\mathbf{2}^{2+}$**@PrS[5]**^{iBu} complex. High binding affinity ($\approx 10^8$ M^{-1}, Table 3) toward $\mathbf{2}^{2+}$ and $\mathbf{3}^{2+}$ was also observed in the presence of bulky cyclohexylethyl and cycloheptylethyl groups at both rims of **PrS[5]**^{EtCy} (Fig. 6g–i†) and **PrS[5]**^{EtcHp} (ESI†), respectively (Table 3).

Conclusions

In this work we report the direct macrocyclization to prism[5] arenes of 2,6-dialkoxynaphthalenes bearing branched and bulky alkyl groups. Utilizing the 1,4-dihexyl-DABCO template, we successfully accomplish the direct macrocyclization of 2,6-dialkoxynaphthalene monomers into prism[5]arene with good yields. This process is effective in the presence of both long and branched alkyl chains. The NMR spectral characteristics of all the synthesized prism[5]arenes, are in accordance with the chiral D_5 symmetry that has been previously reported for other prism[5]arene derivatives. In all cases, DFT calculations indicate that the homochiral all-p*S* (all-p*R*) conformation of **PrS[5]**^{R} as more stable than all the other possible conformations.

The solid state structures of **PrS[5]**^{iPr}, **PrS[5]**^{nBu}, **PrS[5]**^{iBu}, **PrS[5]**^{nPe}, **PrS[5]**^{MeCy}, **PrS[5]**^{EtCy}, and **PrS[5]**^{PrCy} (α- and β- forms) were described. In the solid state, a large opening of the cavity is observed for **PrS[5]**^{iBu}, **PrS[5]**^{MeCy} and the β-form of **PrS[5]**^{PrCy}. The opening observed for **PrS[5]**^{MeCy} and **β-PrS[5]**^{PrCy} can be attributed to the presence of a dichloromethane solvent molecule hosted in the prismarene cavity. In the case of **PrS[5]**^{iBu}, a self-filling effect involving two methyl groups of the alkoxy chains is observed. All molecules crystallize as racemic mixtures of inherent chiral pairs (all-p*S*/all-p*R*) in centrosymmetric space groups. The dynamic stereochemical inversion (from p*R* to p*S* and *vice versa*) behaviour of prism[5] arenes was examined by variable temperature NMR experiments. These studies suggest that the racemization of prism[5] arene derivatives occurs by through-the-annulus rotation of the naphthalene units. With increasing length of linear alkyl substituents from C2 to C9, the chains tend to pack on both rims, thereby diminishing the conformational freedom of the naphthalene units.

The presence of branched alkyl groups at both rims of the prism[5]arenes increases the energy barrier to racemization and consequently lowers the rate of the process. As a result, **PrS[5]**^{iPr} and **PrS[5]**^{iBu} exhibit significantly higher energy barriers to racemization compared to those found for their analogous linear isomers **PrS[5]**^{nPr} and **PrS[5]**^{nBu}. Finally, in prism[5] arenes bearing cyclic units on both rims such as cyclohexylmethyl and cyclohexylethyl, the rotation of the respective 2,6-dialkoxynaphthalene units is blocked on the NMR time scale.

Prism[5]arene derivatives bearing branched or bulky alkyl groups on both rims can form *endo*-cavity complexes with 1,4-dihexyl-DABCO $\mathbf{2}^{2+}$ and piperazonium $\mathbf{3}^{2+}$ guests. **PrS[5]**^{iPr} and **PrS[5]**^{iBu} hosts show higher relative binding affinities toward $\mathbf{2}^{2+}$ and $\mathbf{3}^{2+}$ than those calculated for their linear analogues **PrS[5]**^{nPr} and **PrS[5]**^{nBu}. This result can be justified on the basis of the greater conformational rigidity and preorganization of **PrS[5]**^{iPr} and **PrS[5]**^{iBu} compared to **PrS[5]**^{nPr} and **PrS[5]**^{nBu}.

The knowledge acquired from this study, encompassing the synthesis, structural and conformational properties, as well as the molecular recognition abilities of prism[5]arenes featuring branched and bulky groups at both rims, has the potential to lay the foundation for the development of innovative functional systems based on prismarenes.

Author contributions

The manuscript was written through contributions of all authors.

Conflicts of interest

The authors declare no competing financial interest.

Acknowledgements

C. G. thanks the Italian Ministero dell'Università e della Ricerca (MUR) (PRIN_PNRR P2022XHLTX_PrismaSens) for financial support.

References

1 J.-M. Lehn, Supramolecular Chemistry—Scope and Perspectives Molecules, Supermolecules, and Molecular Devices, *Angew. Chem., Int. Ed. Engl.*, 1988, **27**, 89–112.
2 C. J. Pedersen, Cyclic Polyethers and Their Complexes with Metal Salts, *J. Am. Chem. Soc.*, 1967, **89**, 7017–7036.
3 D. J. Cram, The Design of Molecular Hosts, Guests, and Their Complexes, *Angew. Chem., Int. Ed. Engl.*, 1988, **27**, 1009–1020.

4 P. Neri, J. L. Sessler and M.-X. Wang, *Calixarenes and Beyond*, Springer Int Publishing, 2016.
5 D. J. Cram and J. M. Cram, *Container Molecules and Their Guests*, The Royal Society of Chemistry, Cambridge, 1994.
6 J. Lagona, P. Mukhopadhyay, S. Chakrabarti and L. Isaacs, The Cucurbit[n]uril Family, *Angew. Chem., Int. Ed.*, 2005, **44**, 4844–4870.
7 T. Ogoshi, *Pillararenes*, The Royal Society of Chemistry, Cambridge, 2015.
8 H. Chen, J. Fan, X. Hu, J. Ma, S. Wang, J. Li, Y. Yu, X. Jia and C. Li, Biphen[n]arenes, *Chem. Sci.*, 2015, **6**, 197–202.
9 F. Jia, Z. He, L.-P. Yang, Z.-S. Pan, M. Yi, R.-W. Jiang and W. Jiang, Oxatub[4]arene: A Smart Macrocyclic Receptor With Multiple Interconvertible Cavities, *Chem. Sci.*, 2015, **6**, 6731–6738.
10 J. Li, H.-Y. Zhou, Y. Han and C.-F. Chen, Saucer[n]arenes: Synthesis, Structure, Complexation, and Guest-Induced Circularly Polarized Luminescence Property, *Angew. Chem., Int. Ed.*, 2021, **60**, 21927–21933.
11 (*a*) X.-N. Han, Y. Han and C.-F. Chen, Pagoda[4]arene and *i*-Pagoda[4]arene, *J. Am. Chem. Soc.*, 2020, **142**(18), 8262–8269; (*b*) X.-N. Han, Y. Han and C.-F. Chen, Recent advances in the synthesis and applications of macrocyclic arenes, *Chem. Soc. Rev.*, 2023, **52**, 3265–3298; (*c*) X.-N. Han, Q.-S. Zong, Y. Han and C.-F. Chen, Pagoda[5]arene with Large and Rigid Cavity for the Formation of 1:2 Host–Guest Complexes and Acid/Base-Responsive Crystalline Vapochromic Properties, *CCS Chem.*, 2022, **4**, 318–330.
12 R. Del Regno, P. Della Sala, A. Spinella, C. Talotta, D. Iannone, S. Geremia, N. Hickey, P. Neri and C. Gaeta, Calix[2]naphth[2]arene: A Class of Naphthalene–Phenol Hybrid Macrocyclic Hosts, *Org. Lett.*, 2020, **22**, 6166–6170.
13 L.-P. Yang, X. Wang, H. Yao and W. Jiang, Naphthotubes: Macrocyclic Hosts with a Biomimetic Cavity Feature, *Acc. Chem. Res.*, 2020, **53**, 198–208.
14 P. Della Sala, R. Del Regno, C. Talotta, A. Capobianco, N. Hickey, S. Geremia, M. De Rosa, A. Spinella, A. Soriente, A. Spinella, P. Neri and C. Gaeta, Prismarenes: A New Class of Macrocyclic Hosts Obtained by Templation in a Thermodynamically Controlled Synthesis, *J. Am. Chem. Soc.*, 2020, **142**, 1752–1756.
15 P. Della Sala, R. Del Regno, L. Di Marino, C. Calabrese, C. Palo, S. Geremia, C. Talotta, S. Geremia, N. Hickey, A. Capobianco, P. Neri and C. Gaeta, An intramolecularly self-templated synthesis of macrocycles: self-filling effects on the formation of prismarenes, *Chem. Sci.*, 2021, **12**, 9952–9961.
16 P. Della Sala, R. Del Regno, V. Iuliano, A. Capobianco, C. Talotta, S. Geremia, N. Hickey, P. Neri and C. Gaeta, Confused-Prism[5]arene: a Conformationally Adaptive Host by Stereoselective Opening of the 1,4-Bridged Naphthalene Flap, *Chem. – Eur. J.*, 2023, **29**, e202203030.
17 R. Del Regno, P. Della Sala, N. Hickey, S. Geremia, C. Talotta, P. Neri and C. Gaeta, Insights into the Self-Filling Effects of Branched Isopropyl Groups on the Conformational and Supramolecular Properties of Isopropoxyprism[6]arene, *Eur. J. Org. Chem.*, 2023, e202300608.
18 R. Del Regno, G. D. G. Santonoceta, P. Della Sala, M. De Rosa, A. Soriente, C. Talotta, A. Spinella, P. Neri, C. Sgarlata and C. Gaeta, Molecular Recognition in an Aqueous Medium Using Water-Soluble Prismarene Hosts, *Org. Lett.*, 2022, **24**, 2711–2715.
19 R. Del Regno, P. Della Sala, D. Picariello, C. Talotta, A. Spinella, P. Neri and C. Gaeta, *per*-Hydroxylated Prism[n]arenes: Supramolecularly Assisted Demethylation of Methoxy-Prism[5]arene, *Org. Lett.*, 2021, **23**, 8143–8146.
20 C. Zhai and L. Isaacs, New Synthetic Route to Water-Soluble Prism[5]arene Hosts and Their Molecular Recognition Properties, *Chem. – Eur. J.*, 2022, **28**, e202201743.
21 Q. Song, K. Shang, T. Xue, Z. Wang, D. Pei, S. Zhao, J. Nie and Y. Chang, Macrocyclic Photoinitiator Based on Prism[5]arene Matching LEDs Light with Low Migration, *Macromol. Rapid Commun.*, 2021, **42**, 2100299.
22 Q. Song, K. Zhao, T. Xue, S. Zhao, D. Pei, J. Nie and Y. Chang, Nondiffusion-Controlled Photoelectron Transfer Induced by Host–Guest Complexes to Initiate Cationic Photopolymerization, *Macromolecules*, 2021, **54**, 8314–8320.
23 D. Pei, W. Guo, P. Liu, T. Xue, X. Meng, X. Shu, J. Nie and Y. Chang, Prism[5]arene-based nonporous adaptive crystals for the capture and detection of aromatic volatile organic compounds, *J. Chem. Eng.*, 2022, **433**, 134463.
24 X. Liang, Y. Shen, D. Zhou, J. Ji, H. Wang, T. Zhao, T. Mori, W. Wu and C. Yang, Chiroptical induction with prism[5]arene alkoxy-homologs, *Chem. Commun.*, 2022, **58**, 13584–13587.
25 G. Zhang, Z. Li, Z. Pan, D. Zhao and C. Han, A facile and efficient preparation of prism[6]arene and its dual responsive complexation with 1-adamantane ammonium tetrakis[3,5-bis(trifluoromethyl)-phenyl]borate, *New J. Chem.*, 2023, **47**, 18910–18913.
26 J. Xie, Z. Xi, Y. Yang, X. Zhang, Z. Yang and M. He, Computational investigation of the structures, properties, and host-guest chemistry of prism[n]arenes, *Int. J. Quantum Chem.*, 2023, e27253.
27 T. Ogoshi, K. Masaki, R. Shiga, K. Kitajima and T.-A. Yamagishi, Planar-Chiral Macrocyclic Host Pillar[5]arene: No Rotation of Units and Isolation of Enantiomers by Introducing Bulky Substituents, *Org. Lett.*, 2011, **13**, 1264–1266.
28 N. L. Strutt, H. Zhang and J. F. Stoddart, Enantiopure pillar[5]arene active domains within a homochiral metal–organic framework, *Chem. Commun.*, 2014, **50**, 7455–7458.
29 T. Ogoshi, K. Kitajima, T. Aoki, S. Fujinami, T.-A. Yamagishi and Y. Nakamoto, Synthesis and Conformational Characteristics of Alkyl-Substituted Pillar[5]arenes, *J. Org. Chem.*, 2010, **75**, 3268–3273.
30 M. J. Frisch, G. W. Trucks, H. B. Schlegel, G. E. Scuseria, M. A. Robb, J. R. Cheeseman, G. Scalmani, V. Barone, G. A. Petersson, H. Nakatsuji, X. Li, M. Caricato, A. V. Marenich, J. Bloino, B. G. Janesko, R. Gomperts,

B. Mennucci, H. P. Hratchian, J. V. Ortiz, A. F. Izmaylov, J. L. Sonnenberg, D. Williams-Young, F. Ding, F. Lipparini, F. Egidi, J. Goings, B. Peng, A. Petrone, T. Henderson, D. Ranasinghe, V. G. Zakrzewski, J. Gao, N. Rega, G. Zheng, W. Liang, M. Hada, M. Ehara, K. Toyota, R. Fukuda, J. Hasegawa, M. Ishida, T. Nakajima, Y. Honda, O. Kitao, H. Nakai, T. Vreven, K. Throssell, J. A. Montgomery Jr., J. E. Peralta, F. Ogliaro, M. J. Bearpark, J. J. Heyd, E. N. Brothers, K. N. Kudin, V. N. Staroverov, T. A. Keith, R. Kobayashi, J. Normand, K. Raghavachari, A. P. Rendell, J. C. Burant, S. S. Iyengar, J. Tomasi, M. Cossi, J. M. Millam, M. Klene, C. Adamo, R. Cammi, J. W. Ochterski, R. L. Martin, K. Morokuma, O. Farkas, J. B. Foresman and D. J. Fox, *Gaussian 16, Revision C.01*, Gaussian, Inc., Wallingford CT, 2019.

31 K. Du, P. Demay-Drouhard, K. Samanta, S. Li, T. U. Thikekar, H. Wang, M. Guo, B. van Lagen, H. Zuilhof and A. C.-H. Sue, Stereochemical Inversion of Rim-Differentiated Pillar[5]arene Molecular Swings, *J. Org. Chem.*, 2020, **85**, 11368–11374.

32 R. J. Kurland, M. B. Rubin and M. B. Wise, Inversion Barrier in Singly Bridged Biphenyls, *J. Chem. Phys.*, 1964, **40**, 2426–2427.

33 P. Della Sala, C. Talotta, T. Caruso, M. De Rosa, A. Soriente, P. Neri and C. Gaeta, Tuning Cycloparaphenylene Host Properties by Chemical Modification, *J. Org. Chem.*, 2017, **82**, 9885–9889.

34 C. Gaeta, C. Talotta, L. Margarucci, A. Casapullo and P. Neri, Through-the-annulus threading of the larger calix[8]arene macrocycle, *J. Org. Chem.*, 2013, **78**, 7627–7638.